MAGNETIC FIELDS AND INTENSITY CHANGES IN CORONAL DIMMING REGIONS

G.D.R. Attrill[(1)], N. Narukage[(2)], K. Shibata[(2)], L.K. Harra[(1)]

[(1)]Mullard Space Science Laboratory, University College London, Holmbury St. Mary, Dorking, Surrey, RH5 6NT, UK

Email: gdra@mssl.ucl.ac.uk, lkh@mssl.ucl.ac.uk

[(2)]Kwasan Observatory, Kyoto University, Yamashina, Kyoto, 607-8471, Japan

Email: naru@kwasan.kyoto-u.ac.jp, shibata@kwasan.kyoto-u.ac.jp

ABSTRACT

Examination of the transient coronal holes that appear in conjunction with coronal mass ejections shows that some of these regions drop in intensity to a level that is consistent with the intensity of existing coronal holes. However, other so-called transient coronal holes may dim dramatically, but only to a level close to the intensity level of the quiet sun. The variable timing of the commencement of the dimmings, together with the different intensities of the dimmings, points to the existence of different types of dimming. This study also examines the magnetic field in these dimming regions in order to search for a physical explanation for the different types of dimming that are observed.

1. INTRODUCTION

One particular feature that has been observed when a coronal mass ejection (CME) occurs is a phenomenon known as dimming. Dimming can be observed as a decrease in intensity in both EUV and X-ray images of the solar atmosphere. Dimming regions can appear relatively suddenly on the solar disk and appear to have a good correlation with CME events, in that every dimming event (due to density depletion) has an associated CME event.

The first observation of coronal dimming was made in soft X-rays by the Skylab mission (1973-74). These dimmings were referred to as 'transient coronal holes' (Rust 1983). Since these first early observations, dimmings have also been observed in Yokhoh soft x-ray data (e.g. Sterling & Hudson, 1997) and in SOHO/EIT 195Å extreme ultra violet images (e.g. Thompson et al. 2000).

The cause of these dimmings has been much debated in the literature. There appear to be two main possibilities: Firstly, the dimming may be due to an evacuation of plasma caused by the eruption of the local magnetic field. Following eruption a region of decreased plasma density is left behind. In their study of Doppler motions of the plasma using SOHO/CDS (Coronal Diagnostic Spectrometer) data, Harra & Sterling, 2001, found strong, direct evidence that coronal dimming is indeed due to such plasma evacuation. This work supports the interpretation that there is mass outflow located at the dimming regions. Harrison and Lyons, 2000 came to a similar conclusion based on work that focused on density depletion in coronal dimming regions. Work by Zarro et al. 1999, compared Yohkoh soft x-ray and EIT observations, establishing that dimmings could indeed be caused by a decrease in coronal density.

However, other work (Chertok and Grechnev, 2003; Harrison and Lyons, 2000; Thompson et al. 1998) has highlighted another possible cause of the dimmings. Differences observed between images in different emission lines may suggest that some secondary temperature variations may also be responsible for the appearance of dimmings. Nonetheless, it is generally accepted that coronal dimmings are primarily a result of plasma evacuation.

Dimming observed in the low corona in EUV and X-rays generally begins approximately 30 minutes before the onset of a CME (Thompson et al. 2000) is observed in SOHO/LASCO (Large Angle and Spectrometric Coronagraph) data. The spatial correspondence

Proceedings of the International Scientific Conference on Chromospheric and Coronal Magnetic Fields, 30 August – 2 September 2005 (ESA SP-596, November 2005)

between coronal dimming regions observed in EUV and the angular extent of the associated CME further supports this relationship. This further substantiates the interpretation that coronal dimming regions are indeed primarily due to the evacuation of plasma.

Given the close relationship between the manifestation of coronal dimming regions and CMEs, the drive to understand the magnetism of CMEs naturally requires the investigation of the magnetic nature of dimming regions. This work is motivated by the need to draw a clearer picture of the physical character of coronal dimming regions, particularly with emphasis on their magnetic nature.

This study focuses on a well-observed event which took place on the 10th April 2001. SOHO/EIT observed activity starting in NOAA AR 9415 at 04:48 UT with the area saturating at 05:00 UT. A flare was observed with a coronal "wave" feature spanning much of the solar disk. GOES data reports an X2.3 flare in the same AR beginning at 04:46 UT, with the impulsive phase starting at 05:06 UT. The event also has an associated halo CME.

2. INSTRUMENT DESCRIPTION AND DATA ANALYSIS

This study used SOHO/EIT (Delaboudiniere et al. 1995) 195Å full disk images at approximately 12 minute intervals with a pixel size of 5.26".

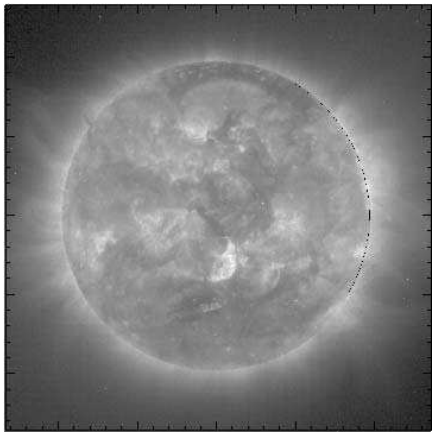

Figure 1 – EIT 195 Å de-rotated image at 06:35 UT on 10th April 2001.

The 195Å bandpass is dominated by Fe XII emission lines at 192.3Å, 193.5Å and 195.1Å, corresponding to a temperature of approximately 1.5 million K at typical coronal densities. We also used data from SOHO/EIT at 171 Å, 284 Å and 304 Å. Fig. 1 shows the EIT 195Å image at 06:35UT. Our data was calibrated using the standard eit_prep routine and for each event, all heliograms were de-rotated to the same pre-event time.

We produced base difference images, where the same pre-event image (at 00:00 UT on 10th April 2001) is subtracted from all subsequent images as well as running difference images where the previous image is subtracted from the following image. The latter were used only as a guide to show the motion of features across the solar disk and the spatial extent of the disturbances. This is because false structures can be created by using the running difference method (see Chertok & Grechnev, 2003).

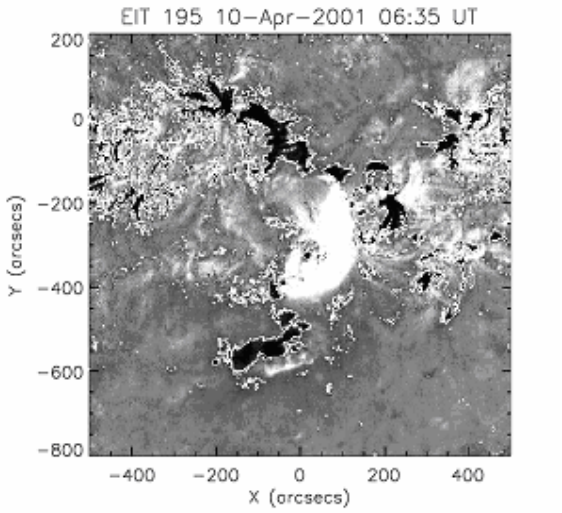

Figure 2a – EIT 195 Å base difference de-rotated image at 06:35 UT with overplot of contours defining the dimming regions.

2.1 Defining the dimming regions

We define the dimming regions using the base difference images. We used the percentage difference between the maximum quiet Sun level and the minimum coronal hole level. If this was more than 50% then it was defined as a region of dimming. (Fig. 2a shows the base difference image near the time of maximum dimming with the contours overlaid).

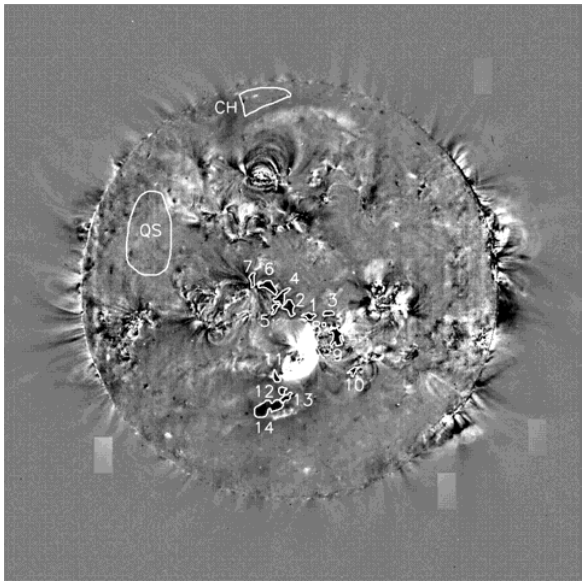

Figure 2b – EIT 195 Å full disk base difference de-rotated image at 06:35 UT with overplot of selected dimming regions as shown in Figure 2a. The figure also shows the selected quiet sun (QS) and polar coronal hole (CH) regions selected for comparison.

We then created light-curves from the original image (not the difference image) of the selected dimming regions in order to be able to measure quantitatively the time variation in the emission. The light-curves therefore show the EUV intensity averaged over each dimming region.
In addition, we examined a polar coronal hole as well as an undisturbed 'quiet sun' area of the solar disk in order to make comparisons to the dimming regions.

SOHO/MDI (Scherrer et al. 1995), full disk magnetograms with a 96-minute cadence and a pixel size of 1.98" provided the magnetic data used in this study.
The magnetogram that was closest in time to the strongest dimming was used to measure the magnetic flux for each region. The appropriate magnetogram was rotated to match the rotation correction made for the EIT images.
We measured the total magnetic flux through each dimming region. We were then able to calculate the positive, negative and net flux in each region. We define the net flux as the magnitude of the flux of the dominant polarity in a given region minus the magnitude of the opposite polarity flux in that region.

The MDI data was also corrected for radial projection effects using the standard zradialize routine.

The H-Alpha data used in this study was provided by the Hida Flare Monitoring Telescope (FMT) (Kurokawa et al. 1995). The FMT observes four full-disk images in the H-alpha line centre ± 0.8Å and continuum.
The data have a cadence of 1 minute, a pixel size of 4.”2 and were processed using the flare monitoring telescope standard procedures. Where comparison with spacecraft data is made, the ground based data is corrected to align correctly with the spacecraft data.

Full-disk AlMg and thin Al filter SXT data from Yohkoh (Tsuneta et al. 1991) were calibrated according to standard procedure using sxt_prep. The SXT data pixel size is 2”.46 . The intensity per pixel was normalized to the exposure duration.

2.2 Analysis of the event

We applied the de-rotation method from 00:00 UT on 10th April 2001 until approximately 10:00 UT on 11th April 2001 before limb brightening/darkening effects due to the de-rotation encroached on disk centre where the main dimming regions are located. After 10:00 UT on 11th April 2001, the data is deemed unusable. Fig. 1 shows the EIT image. The dimming regions can be seen in the vicinity of the flaring region. In addition, the north coronal hole and a region of quiet Sun were also analysed in order to compare the changes to a 'steady state feature', undisturbed by the eruption. The regions chosen are shown in Fig. 2b.

Having defined the dimming regions, we checked to see if the dimmings were due to a density or temperature effect. By comparing data at different wavelengths (namely; Yohkoh SXT AlMg, SoHO/EIT 171Å, 284Å & 304Å), it is apparent that the overall morphology of the dimming is evident at the different wavelengths, hence the dimming can be confirmed as a product of density change in this event.

The light-curves of the EUV intensity averaged over each dimming region enable us to study the evolution of the EUV intensity.

These light-curves show that regions 2, 12, 13 & 14 dim to a level where their intensity is at or just below that of the north polar coronal hole. Regions 1, 3, 4, 6 & 11 dim to a level between the quiet sun and coronal hole intensity. Whilst regions 5, 7, 8, 9, & 10 dim to various levels above the intensity of the quiet sun. The dimmings of regions 1, 2, 10 & 14 do not recover to a level near to their pre-event intensity level within our dataset, although (with the exception of region 10), they do show a steady recovery.

2.3 Magnetic flux balance

Using SOHO/MDI data we measured the magnetic flux through each dimming region and found that regions 1,2,4,5,6 & 7 have a net negative flux and the remaining regions have a net positive flux. Fig. 3 shows the net polarity in each region.

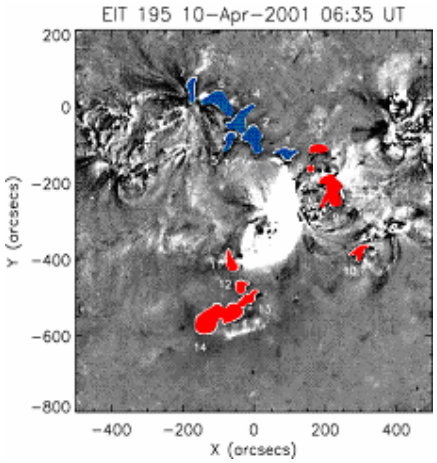

Figure 3 shows the net polarity of the magnetic flux through each dimming region. Blue indicates a region of net negative polarity and red indicates a region of net positive polarity.

The total positive flux through all of the dimming regions is found to be 1.8×10^{21}Mx and the total negative flux is -1.5×10^{21}Mx. These flux measurements are suggestive of the magnetic structure of the loop systems, in that a flux balance implies a closed, balanced, self-contained system.

2.4 Light-curves and interconnectivities

Examination of the light-curves indicates that the EUV emission from dimming regions of opposite polarity exhibit a similar evolution. For example, the light-curves of regions 2, 12 and 13 when superimposed (see Fig. 4) clearly all have a similar intensity evolution and dim to the existing polar coronal hole level. Further, the total positive flux through these regions is 8×10^{19}Mx and the total negative flux is -8×10^{19}Mx.

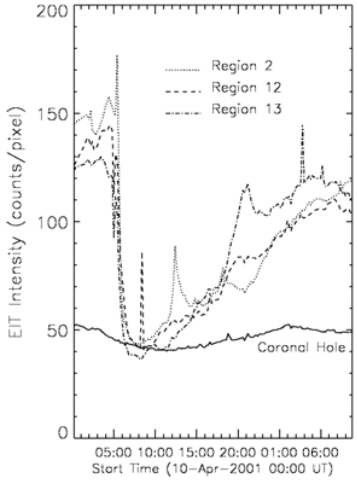

Figure 4 shows a superposition of the light-curves of regions 2, 12 & 13. Note that all the regions dim to coronal hole level and exhibit a similar intensity evolution.

This similar evolution between light-curves of regions of opposite polarity is repeated for many of the dimming regions. In particular, the gradient of the recovery phase (from the point of the maximum dimming onward) is a quantitative measure that emphasizes this point. See Tab. 1.

Table 1 shows the recovery phase gradient for various dimming regions. Blue indicates a region of net negative magnetic flux and red a net positive flux.

Regions	Recovery Phase Gradient (counts per pixel/second)
1 & 14	0.0004 & 0.0004
2 & 12 & 13	0.0008 & 0.0008 & 0.0010
3 & 4	0.0016 & 0.0017
6 & 8 & 9	0.0025 & 0.0021 & 0.0024

From all the light-curves, two signatures in particular show a significantly different evolution to the others. The light-curves of regions 5 and 11 exhibit a relatively

fast, sharp recovery (see Fig. 5).

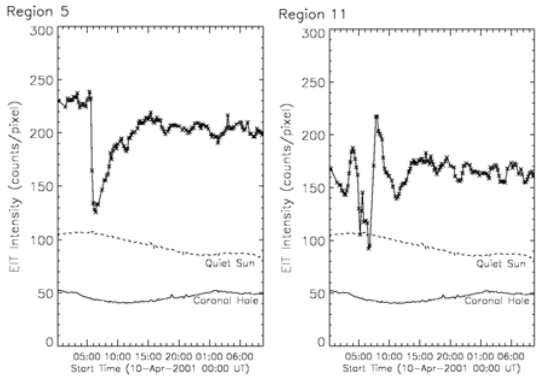

Figure 5 shows the EUV emission light-curves of regions 5 & 11. These are the only two dimming regions of the 14 identified to exhibit a fast, sharp recovery. The dashed (solid) line is the quiet sun (north polar coronal hole) intensity level.

Region 5 has a net negative polarity and region 11 a net positive polarity. The point of maximum dimming (the lowest intensity level of the light-curves) of regions 5 and 11 occur at 06:23 UT and 06:35 UT respectively. Both regions dim to a level near to that of the quiet sun intensity level.

An overlay of these two regions (see Fig. 6) on a Yohkoh AlMg image map at 06:32 UT shows that the apparent ends of the SXT feature terminate near to the boundaries of these two EUV dimming regions.

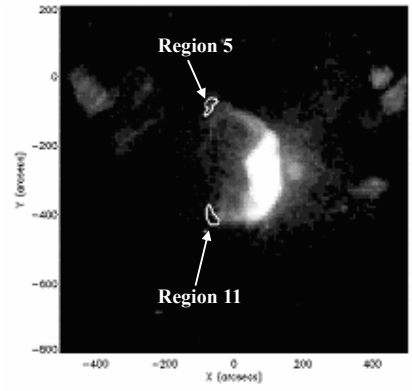

Figure 6 - A Yohkoh AlMg image map at 06:32 UT with the location of dimming regions 5 and 11 superimposed. The apparent ends of the SXT feature appear to terminate near to the boundaries of these two EUV dimming regions.

2.5 Sharp brightening signature

Some of the light-curves show a distinct spike, a sharp increase in intensity just before the sharp drop in intensity that indicates the dimming process. (Eg. Fig.4 shows such a sharp increase in the light-curve for region 2, between 05:00 and 06:00 UT on 10th April 2001). Examination of the H-alpha data around the time of this sharp increase in intensity in EIT 195 Å suggests that a bright surge connected with the flaring region may be responsible for this observed brightening. In the light-curve of region 2, the peak of this increase in intensity is observed at 05:23 UT. Overlaying the location of region 2 on the H-alpha data (see Fig. 7) shows that the bright surge in H-alpha passes beneath the location of this region between 05:18 and 05:25 UT.

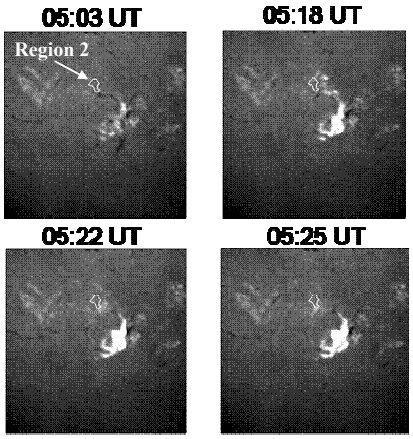

Figure 7 details the H-alpha data showing the bright surge. The location of dimming region 2 is overlaid to illustrate that the bright surge passes underneath the location of this region between 05:18 and 05:25 UT.

3. DISCUSSION

Examination of the light-curves reveals many different types of evolution of the EUV intensity in the dimming regions. Chertok & Grechnev, 2004 present an interesting interpretation for these different types of dimmings. They suggest that the rapid re-formation of certain coronal structures suggests that some of the dimmings may not have resulted from the actual opening of coronal field into the solar wind. Instead, some of the coronal restructurings that are observed may have corresponded to partial eruptions, in which a homologous contraction followed the event-related

expansion of the structure.

It is also apparent that other dimmings are indeed related to the actual opening of the magnetic field. The brightening observed in H-alpha may provide supporting evidence for such an argument. The brightening in H-alpha is caused by hot plasma, which is heated by the reconnection process during the observed flaring activity. Given that this bright surge passes right beneath the location occupied by region 2 in EIT 195 Å data (see Fig. 6), between 05:18 and 05:25 UT, it is speculated that the sharp increase in EUV intensity observed at 05:23 UT is most likely associated with the brightening observed in H-alpha at this time.
The main dimming process (due to plasma evacuation) must take place when the magnetic field is open. The decrease in intensity of the EUV light-curves immediately after the sharp increase in EUV intensity indicates the manifestation of this dimming process.
It is suggested that the brightening observed in EUV, given its close association (both spatially and temporally) with the brightening observed in H-alpha, is an indirect signature of the magnetic reconnection process. The argument for this is that brightenings seen in H-alpha are due to heating of the plasma and such intense heating is a by-product of magnetic reconnection.

The light-curves show that the dimming proceeds until it reaches a maximum (the EUV intensity drops to a minimum) and then the intensity level starts to recover. The fact that the light-curves show a recovery would suggest that plasma re-accumulates in these dimming regions, providing the increase in intensity that we observe. For there to be an increase in intensity (a recovery) there must be an accumulation of plasma (to emit the intensity that we see). Whilst the magnetic field remains open, the plasma is subject to evacuation or dissipation. It is only when the magnetic field closes that the plasma can re-accumulate, creating what we observe as an increase in intensity.

A further point of interest is the flux balance between the magnitude of the total positive and total negative flux from all of the selected dimming regions.
The total positive flux is found to be 1.83e+21 Mx and the total negative flux is found to be -1.53e+21 Mx. These flux measurements are suggestive of the magnetic structure of the loop systems, in that a flux balance implies a closed, balanced, self-contained system.

4. CONCLUSION

This multi-wavelength study shows that the dimmings associated with the eruptive activity on 10th April 2001 from AR 9415 are indeed due to a change in density and can therefore be interpreted in the context of plasma evacuation. An approximate magnetic flux balance is found between all of the identified dimming regions, implying a closed, balanced, self-contained system.

Similarities in the evolution of the EUV emission from regions of opposite polarity may give information about the magnetic structure of the eruption region. The two fast recovery signatures (namely regions 5 and 11) appear to be associated with the dimming regions at the termination points of the SXT feature.
Finally, careful examination and interpretation of the EUV light-curve intensity evolution in the dimming regions provides us with a diagnostic tool for determining the timescale over which the magnetic reconnection process takes place.

5. REFERENCES

Chertok, I. M. & Grechnev, V. V., *J. Geophys. Res*., 109, 2112, 2004.

Chertok, I. M. & Grechnev, V. V., *Astron. Reports*, 47, 2, 139, 2003.

Delaboudiniere, J. P. et al., *Sol. Phys*, 162, 129, 1995.

Harra, L. K. & Sterling, A. C., *ApJ*, 561, L215, 2001.

Harrison, R. A. & Lyons, M., *A&A*, 358, 1097, 2000.

Kurokawa, H. et al., J. *Geomag Geoelectr*, 47, 1043, 1995.

Rust, D. M., *Space Science Rev*., 34, 21-36, 1983.

Scherrer P. H. et al., *Sol. Phys*, 162, 129, 1995.

Sterling, A. C. & Hudson, H. S., *ApJ*, 491, L55-L58, 1997.

Thompson, B. J. et al, *GRL*, 27, 10, 1431, 2000.

Thompson, B. J. et al, *GRL*, 25, 2465, 1998.

Tsuneta, S. et al., *Sol. Phys*, 136, 37, 1991.

Zarro, D. M. et al., *ApJ*, 520, L139-L142, 1999.